Original Article

Modulations of the mTORC2–GATA3 axis by an isorhamnetin activated endosomal–lysosomal system of the J774.1 macrophage-like cell line

Maiko Sakai,[1] Kohta Ohnishi,[1,*] Masashi Masuda,[1] Erika Harumoto,[1] Teppei Fukuda,[1] Aika Ohnishi,[1] Shunsuke Ishii,[2] Hirokazu Ohminami,[1] Hisami Yamanaka-Okumura,[1,3] Kazuto Ohashi,[4] Eisuke Itakura,[5] Kazuki Horikawa,[6] Shigenobu Yonemura,[7,8] Taichi Hara,[9] and Yutaka Taketani[1,*]

[1]Department of Clinical Nutrition and Food Management, Institute of Biomedical Sciences, [6]Department of Optical Imaging, Advanced Research Promotion Center, and [7]Department of Cell Biology, Tokushima University Graduate School of Medical Nutrition, 3-18-15 Kuramoto-cho, Tokushima-shi, Tokushima 770-8503, Japan
[2]Department of Biology, Graduate School of Science and Engineering and [5]Department of Biology, Graduate School of Science, Chiba University, 1-33 Yayoi-cho, Inage-ku, Chiba 263-8555, Japan
[3]Department of Food Science and Nutrition, Doshisha Women College of Liberal Arts, Teramachi-Nishi-iru, Imadegawa-Kamigyo-ku, Kyoto 602-0893, Japan
[4]Institute for Molecular and Cellular Regulation, Gunma University, 3-39-15 Showa-cho, Maebashi-shi, Gunma 371-8512, Japan
[8]Laboratory for Ultrastructural Research, Riken Center for Biosystems Dynamics Research, 2-2-3 Minatojimaminami-machi, Chuo-ku, Kobe-shi, Hyogo 650-0047, Japan
[9]Laboratory of Food and Life Science, Faculty of Human Sciences, Waseda University, 2-579-15 Mikajima, Tokorozawa-shi, Saitama 359-1192, Japan

(Received 6 February, 2024; Accepted 12 March, 2024; Released online in J-STAGE as advance publication 20 March, 2024)

The endosomal–lysosomal system represents a crucial degradation pathway for various extracellular substances, and its dysfunction is linked to cardiovascular and neurodegenerative diseases. This degradation process involves multiple steps: (1) the uptake of extracellular molecules, (2) transport of cargos to lysosomes, and (3) digestion by lysosomal enzymes. While cellular uptake and lysosomal function are reportedly regulated by the mTORC1–TFEB axis, the key regulatory signal for cargo transport remains unclear. Notably, our previous study discovered that isorhamnetin, a dietary flavonoid, enhances endosomal–lysosomal proteolysis in the J774.1 cell line independently of the mTORC1–TFEB axis. This finding suggests the involvement of another signal in the mechanism of isorhamnetin. This study analyzes the molecular mechanism of isorhamnetin using transcriptome analysis and reveals that the transcription factor GATA3 plays a critical role in enhanced endosomal–lysosomal degradation. Our data also demonstrate that mTORC2 regulates GATA3 nuclear translocation, and the mTORC2–GATA3 axis alters endosomal formation and maturation, facilitating the efficient transport of cargos to lysosomes. This study suggests that the mTORC2–GATA3 axis might be a novel target for the degradation of abnormal substances.

***Key Words*: protein degradation, endocytosis, GATA3, mTORC2, isorhamnetin**

Organisms continuously synthesize thousands of proteins following the central dogma of survival, growth, and reproduction. However, endogenous and exogenous stresses can lead to *in vivo* aberrant alterations in protein structures, such as misfolding, carbonylation, and glycation.[1–4] Several intracellular proteolytic machineries, including autophagy for intracellular substrates and the endosomal–lysosomal system for extracellular substrates, address these stresses.[5,6] Dysfunction of these principal degradation systems results in the accumulation of abnormal macromolecules closely associated with the onset of various disorders, including neurodegenerative, cardiovascular, and autoimmune diseases.[7–10] While the molecular mechanisms underlying autophagy regulation have been vigorously elucidated,[11,12] mechanism-based strategies for controlling the endosomal–lysosomal system are yet to be fully established.

The endosomal–lysosomal pathway comprises multiple steps: uptake of extracellular molecules, transport of cargo to lysosomes, and degradation by lysosomal hydrolases.[13,14] The transcription factor EB (TFEB) is a well-known master regulator of lysosomal biogenesis and function. Macrophage-specific overexpression of TFEB enhances lysosomal-related genes and suppresses atherosclerosis in ApoE-knockout mice.[15] Genes related to endocytic receptors, caveolin, and clathrin adaptor are also regulated by TFEB, and TFEB overexpression promotes the uptake of extracellular molecules.[16] However, a pivotal regulator of cargo transport to lysosomes, along with endosome formation and maturation, has not been elucidated, presenting a potential breakthrough in the pharmacological regulation of the endosomal–lysosomal system.

Macrophages engulf and digest a broad range of extracellular macromolecules, such as infectious bacteria and apoptotic cells, making the elucidation of the regulators of this system especially critical. In a previous study, we screened a dietary polyphenol capable of enhancing endosomal–lysosomal degradation in the J774.1 macrophage-like cell line and identified isorhamnetin,[17] a natural flavonol in potherb mustards, apple, and radish leaves, as a potent activator.[18] We investigated whether isorhamnetin induces TFEB transactivation, revealing unknown mechanisms independent of the mammalian target of rapamycin (mTOR) complex1 (mTORC1)-TFEB signal. This study analyzes the molecular mechanism underlying the enhancement of endosomal–lysosomal proteolysis by isorhamnetin in J774.1 cells. Informatics challenges on comprehensive data from transcriptome and immunocytochemical experiments led to the identification of the mTOR complex2 (mTORC2)–GATA-binding protein 3 (GATA3) signal as a novel regulator of endosome formation and maturation, contributing to the endosomal–lysosomal pathway.

*To whom correspondences should be addressed.
E-mail: kohta_ohnishi@yahoo.co.jp (KO); taketani@tokushima-u.ac.jp (YT)

doi: 10.3164/jcbn.24-22

Materials and Methods

Reagents. Bovine serum albumin (BSA; 01281-26) was purchased from Nacalai Tesque, Inc. (Kyoto, Japan). Antibodies against phospho-Akt (Ser473) (4058), GATA-3 (5852), phospho-4E-BP1 (Thr37/46) (7547), and EEA1 (48453) were purchased from Cell Signaling Technology Inc. (Danvers, MA). Antibody to β-Actin (sc-4778) was purchased from Santa Cruz Biotechnology, Inc. (Dallas, TX). The Rab7 (ab137029) antibody was obtained from Abcam Inc. (Cambridge, UK). Torin1 (10997) was purchased from Cayman Chemical Co. (Ann Arbor, MI). Isorhamnetin (1120S) and tamarixetin (1140S) were purchased from ExtraSynthese (Genay, France). JR-AB2-011 (HY-122022) was purchased from MedChem Express (Monmouth Junction, NJ).

Cell culture. J774.1, mouse macrophage-like cell line, was obtained from American Type Culture Collection. They were cultured as previously described.[17]

Prediction of transcription factors relating to isorhamnetin activity. Total RNA was isolated from the cells using Sepasol-RNA I Super G (09379-55; Nacalai Tesque). The quality and concentration of the RNA were checked using a 2100 Bioanalyzer (Agilent Technologies, Palo Alto, CA), and the gene expression profile was analyzed using an Agilent gene expression microarray (SurePrint G3 Mouse GE Microarray Kit 8 × 60 K, ver. 2; Agilent Technologies). Principal component analysis was performed using the GeneSpring GX software (Tomy Digital Biology, Tokyo, Japan). Enrichment analysis of transcription factors was performed using the Genomatix Software Suite (https://www.genomatix.de/solutions/genomatix-software-suite.html). The criteria for differentially screening expressed mRNA was fold change >1.5 or <−1.5.

DQ-BSA degradation assay. The DQ-BSA degradation assay was performed as previously described using an Operetta high-content imaging system (PerkinElmer, Waltham, MA).[17]

Generation of knockout cells using the CRISPR/Cas9 system. The 20-nucleotide guide sequences targeting mouse *GATA3*, *raptor*, and *rictor* were designed using the CCTop—CRISPR/Cas9 target online predictor (https://cctop.cos.uni-heidelberg.de:8043/). Two types of gRNA were designed for each gene.

GATA3: 5'-CTTCCATGTACGAATGGCCG-3' (Exon2),
5'-CTACTACGGAAACTCCGTCA-3' (Exon2)
raptor: 5'-GTCGCCTCTTATGGGACTCG-3' (Exon1),
5'-CCAAATCTTTAGCGCAGAGC-3' (Exon1)
rictor: 5'-GCCAACTCATTAATTGCGGT-3' (Exon7),
5'-GGTGTTTAGTCCTCCTCGAA-3' (Exon8)

These oligo-DNAs were cloned into pSpCas9 (BB)-2A-Puro (PX459) V2.0 (#62988; Addgene, Cambridge, MA). The ligated plasmid was transfected to J774.1 cells by electroporation using a NEON Transfection System (Thermo Fisher Scientific, Waltham, MA) at 1,600 V for 10 ms (two pulses were serially added). The transfected cells were incubated in DMEM (10% FBS, PS-free) for 24 h, and then selected by puromycin at a final concentration of 8 μg/ml for 24 h. After growing cells for 2 days, the cells were serially diluted onto 96-well plates to obtain single-cell colonies. Single clones were expanded and screened for each target protein by Western blotting.

Confirmation of GATA3-knockout by sequencing gDNA. The single clones obtained in the CRISPR/Cas9 methodology were expanded and screened for GATA3 mRNA expression by RT-qPCR. Then, the clones with significantly lower GATA3 expression were selected, and the genomic DNA was extracted as follows. Cells were collected with PBS, resuspended in TNE buffer containing 0.72% SDS and proteinase K (320 ng/ml), and purified by phenol/chloroform extraction and NaOAc/ethanol precipitation. Then, the DNA was subjected to PCR using a primer set (forward 5'-GAGGACATGGAGGTGACTGC-3', reverse 5'-GATACCTCTGCACCGTAGCC-3') to amplify the exon-2 region containing the gRNA sequence in the GATA3 locus.

Immunocytochemistry. Ice-cold PBS was used to wash the cells. The cells were fixed with 4% paraformaldehyde for 5 min at room temperature and washed twice. Cells were permeabilized with 0.1% Triton X-100 (35501-02; Nacalai Tesque) for 5 min, followed by two washes. The cover slips were blocked with 0.8% BSA for 30 min at room temperature and incubated with antibodies (1:100) diluted in 0.8% BSA for 1 h. They were washed twice with 0.8% BSA and incubated with secondary antibodies (diluted 1:100) and Hoechst33342 (1 μg/ml) in the dark for 1 h at room temperature. After washing thrice with 0.4% BSA, the cover glasses were washed twice and adhered to glass slides using Dako Fluorescent Mounting Medium (DAKO, Carpinteria, CA). Images were obtained using a confocal microscope (A1R HD25; Nikon, Tokyo, Japan). The stained areas were quantified using ImageJ software.

Western blotting. Western blotting was performed as previously described.[17]

RNA sequencing. Total RNA was isolated from the cells using the RNeasy Plus Mini Kit (74134; Qiagen, Hilden, Germany) and submitted to Filgen (Aichi, Japan) for RNA-sequencing sequencing (paired-end 150 bp). Clean data were obtained by filtering raw data as follows: (1) discard reads containing adapters, (2) discard reads containing >10% undetermined bases, and (3) discard reads containing >50% low-quality bases. The clean data were aligned to the GRCm38 genome, and the gene expression values (TPM) were calculated using the CLC Genomics Workbench ver. 20.0.4 (QIAGEN, Tokyo, Japan). Gene Ontology (GO) enrichment analysis was performed using the DAVID Bioinformatics Resources 6.8.

Measurement of endosomal acidification. Cells were incubated with pHrodo Red dextran (P10361; Invitrogen) (40 μg/ml) for 10 min. After washing with FluoroBrite DMEM three times, red fluorescence inside cells was imaged and quantified using the Operetta high-content imaging system with a 40× objective lens (λ ex: 530–560 nm, λ em: 570–650 nm).

Transmission electron microscopy. Cells were incubated with 10 mg/ml horseradish peroxidase (HPOD; Funakoshi, Tokyo, Japan) for 10 min to characterize the endocytic vesicles by electron microscopy. The cells were fixed in 2% glutaraldehyde in 0.1 M sodium cacodylate buffer (pH 7.4) for 1 h. After washing, horse radish peroxidase (HRP) was visualized by incubating the cells in 0.5 mg/ml diaminobenzidine (FUJIFILM Wako, Osaka, Japan) in the same buffer containing 0.03% H_2O_2 for 15 min on ice.[19] After washing, the cells were post-fixed with 1% OsO_4 in the same buffer for 30 min on ice. After block-staining with uranyl acetate overnight, samples were dehydrated with ethanol and embedded in Epon 812 resin (TAAB, Aldermaston, UK), polymerized at 60°C for 2 days, and ultra-thin sections (thickness, 70 nm) were cut using an ultramicrotome (EM-UC6; Leica Microsystems, Wetzlar, Germany), placed on copper grids, doubly stained with uranyl acetate and lead citrate, and examined on a JEM 1400 Plus electron microscope (JEOL) at 100 kV.

Quantification of lysosomal degradation activity. Lysosomal-METRIQ probes were used to measure the lysosomal degradation activity. HEK293FT cells were transiently co-transfected with pCW57.1 Lysosomal-METRIQ (31), pCMV-VSVG (Addgene, #8454), and psPAX2 (Addgene, #12260) using PEI MAX reagent (Polysciences, Warrington, PA). After culturing for 72 h, a growth medium containing the lentivirus was collected. J774.1 cells were transfected with tTS/rtTA_M2 (VectorBuilder, VB160419-1020 mes) using Xfect transfection reagent (631317; Takara Bio, Shiga, Japan), and neomycin-resistant cells were selectively cultured for 10 days. The cells were then subjected to single-cell sorting, and a single clone strongly expressing tTS/rtTA mRNA was screened by RT-qPCR. The J774.1 Tet-On cells were incubated with lentivirus-

containing medium with 10 mg/ml polybrene for 24 h, and then selected by puromycin (5 μg/ml) for 2 weeks to obtain a stable cell line. The J774.1 Tet-On cells harboring the lysosomal-METRIQ probe were incubated with doxycycline (1 μg/ml) for 24 h and treated with IR (10 μM) or rapamycin (1 μM) for another 24 h. After washing with FluoroBrite DMEM twice, the cellular fluorescence of mCherry and GFP was imaged using the Operetta high-content imaging system with a 40× objective lens (λ ex: 530–560 nm, λ em: 570–650 nm for mCherry; λ ex: 460–490 nm, λ em: 500–550 nm for GFP). mCherry/GFP signal ratios, reflecting the lysosomal degradation activity, are shown in the graphs.

Measurement of cellular uptake of dextran. Cells were seeded in black-walled clear-bottomed 96-well plates and treated with isorhamnetin (10 μM) or rapamycin (1 μM) for 24 h. To measure cellular uptake activity, cells were incubated with FITC-Dextran MW 70,000 (46945; Sigma-Aldrich) (1 mg/ml) for 2 h. The cells were washed with PBS twice and fixed with 2% paraformaldehyde for 5 min. After washing with FluoroBrite DMEM twice, green fluorescence inside cells was imaged and quantified in the manner described in the DQ-BSA degradation assay.

Statistical analyses. All data were expressed as the means ± SEM. Statistical analyses were performed using one-way analysis of variance (ANOVA). The groups were compared using the Tukey–Kramer test when ANOVA indicated a significant difference among the groups, The threshold for statistical significance was set at $p<0.05$.

Results

GATA3 is a critical transcription factor for activated endosomal–lysosomal degradation by isorhamnetin. Our previous study found that isorhamnetin strongly activated endosomal–lysosomal proteolysis in J774.1 cells using the DQ-BSA protein, a reagent designed to be endocytosed and degraded in lysosomes with fluorescence emission. A previous study also found a significant involvement of transcriptional regulation;[17] therefore, we performed a microarray analysis of gene expression. Torin1 is an mTOR inhibitor that strongly activates DQ-BSA protein degradation. Therefore, it was used as a positive control, and tamarixetin (an inactive isomer of isorhamnetin) was used as a negative control (Supplemental Fig. 1A*). Principal component analysis was used to visualize the transcriptomes that were altered by isorhamnetin, tamarixetin, or Torin1 (Fig. 1A). Genes whose expression was altered (fold change >1.5) were extracted, and transcription factors were predicted to be regulated by each treatment (Fig. 1B). Venn diagrams show the number of candidate transcription factors, indicating that the five transcription factors were activated by isorhamnetin and Torin1 but not by tamarixetin. Gene editing experiments using the CRISPR/Cas9 system revealed that the knockout of GATA3 (one of the five candidates) significantly decreased the effects of isorhamnetin on DQ-BSA degradation (Supplemental Fig. 1B, C*, and Fig. 1C). This result was confirmed in two different GATA3 knockout clones, and clone 1 was used for subsequent experiments. We subsequently investigated the nuclear translocation of GATA3 and found that isorhamnetin or Torin1 treatment increased GATA3 levels in the nucleus (Fig. 1D). These data suggest that GATA3 is regulated by isorhamnetin and promotes endosomal–lysosomal proteolysis.

Inhibition of mTORC2 signaling by isorhamnetin promotes GATA3 transactivation. Torin1 is an mTOR inhibitor that targets mTORC1 and mTORC2 and activates GATA3 nuclear translocation (Fig. 1D). We predicted that GATA3 is regulated by either mTORC1 or mTORC2 signaling. We evaluated the effects of isorhamnetin on mTORC1 and mTORC2 activities by detecting the phosphorylation of 4E-BP1 and Akt (Ser473), respectively. Isorhamnetin markedly suppressed Akt phosphorylation, whereas the phosphorylation level of 4E-BP1 was hardly altered, similar to the effects of JR-AB2-011, a selective mTORC2 inhibitor (Fig. 2A). Therefore, we attempted to elucidate the relationship between mTORC2 and GATA3 expression. We generated *rictor*-knockout J774.1 cells lacking mTORC2 activity (Supplemental Fig. 2A*) and observed the cellular localization of GATA3. We found that *rictor*-knockout interrupted its nuclear translocation by isorhamnetin, and its localization shifted to the cytoplasm by *rictor*-knockout even under unstimulated conditions (Fig. 2B), suggesting that the transactivation of GATA3 is controlled by mTORC2 signaling. Unexpectedly, the depletion of *rictor* led to the accumulation of GATA3 in the cytoplasm in DMSO treated control cells, suggesting that the cells may have adapted to the *rictor* deficiency, activating compensatory mechanisms. Subsequently, we generated *raptor*-knockout J774.1 cells lacking mTORC1 activity (Supplemental Fig. 2B*) and evaluated the effects of *raptor* or *rictor*-knockout on the activation of DQ-BSA proteolysis by isorhamnetin; its activity was only inhibited in *rictor*-deficient cells (Fig. 2C). Furthermore, we confirmed JR-AB2-011 enhanced DQ-BSA degradation, indicating that the inhibition of mTORC2 promotes endosomal–lysosomal proteolysis (Supplemental Fig. 2C*). Additionally, Torin1 treatment of *rictor*-deficient cells failed to enhance DQ-BSA degradation, whereas *raptor*-knockout cells showed a similar response to wild type cells (Supplemental Fig. 2D*). These data suggest that isorhamnetin acts on the mTORC2–GATA3 axis, which is a critical regulator of endosomal–lysosomal degradation.

GATA3 regulates endosomal formation and maturation via gene expression relating to endosomes. We performed a comprehensive analysis of gene expressions in *GATA3*-knockout cells by RNA-seq to investigate the molecular mechanism by which GATA3 regulates endosomal–lysosomal degradation. Most of the genes that were upregulated or downregulated by isorhamnetin treatment (fold change >1.5) in wild-type cells were not altered in *GATA3*-knockout cells (Fig. 3A). Subsequently, GO enrichment analyses were performed on the GATA3-dependent gene set altered by isorhamnetin treatment. Several GO terms exhibited significant enrichment, with a focus on those associated with the endosomal–lysosomal system, identifying "lysosomes" and "cytoplasmic vesicles" (Fig. 3B). Notably, experiments using a lysosomal METRIQ probe indicated that isorhamnetin did not affect lysosomal activity (Supplemental Fig. 3A*). We subsequently focused on the "cytoplasmic vesicle" and analyzed more concrete terms that revealed that GO terms of the "endosome" were most significantly enriched (Fig. 3B).

In the endosomal–lysosomal system, early endosomes containing substrates are formed and subsequently mature into late endosomes, which are essential for the transport of cargo to lysosomes. To visualize endosomes, cells were stained with EEA1 for early endosomes and Rab7 for late endosomes. Interestingly, the EEA1 area was significantly enhanced by pretreatment with isorhamnetin, which revealed that endosome formation was enhanced by isorhamnetin (Fig. 3C). Furthermore, the Rab7 area and co-localized puncta representing endosomes in the middle of the conversion from early to late endosomes were also increased by isorhamnetin treatment (Fig. 3C). These findings indicate that the increased early endosomes smoothly mature into late endosomes. In the endosomal–lysosomal pathway, vesicular pH decreased with maturation, and we found that isorhamnetin significantly enhanced endosome acidification (Fig. 3D). Additionally, transmission electron microscopy revealed a significant enlargement of endocytic vesicles detected by HRP staining in isorhamnetin-treated cells, suggesting that isorhamnetin increased the size of endosomes (Fig. 3E). These results indicate that isorhamnetin promotes the formation and maturation of endosomes with increasing size, which could enable the efficient transport of cargo to lysosomes.

*See online. https://doi.org/10.3164/jcbn.24-22

doi: 10.3164/jcbn.24-22

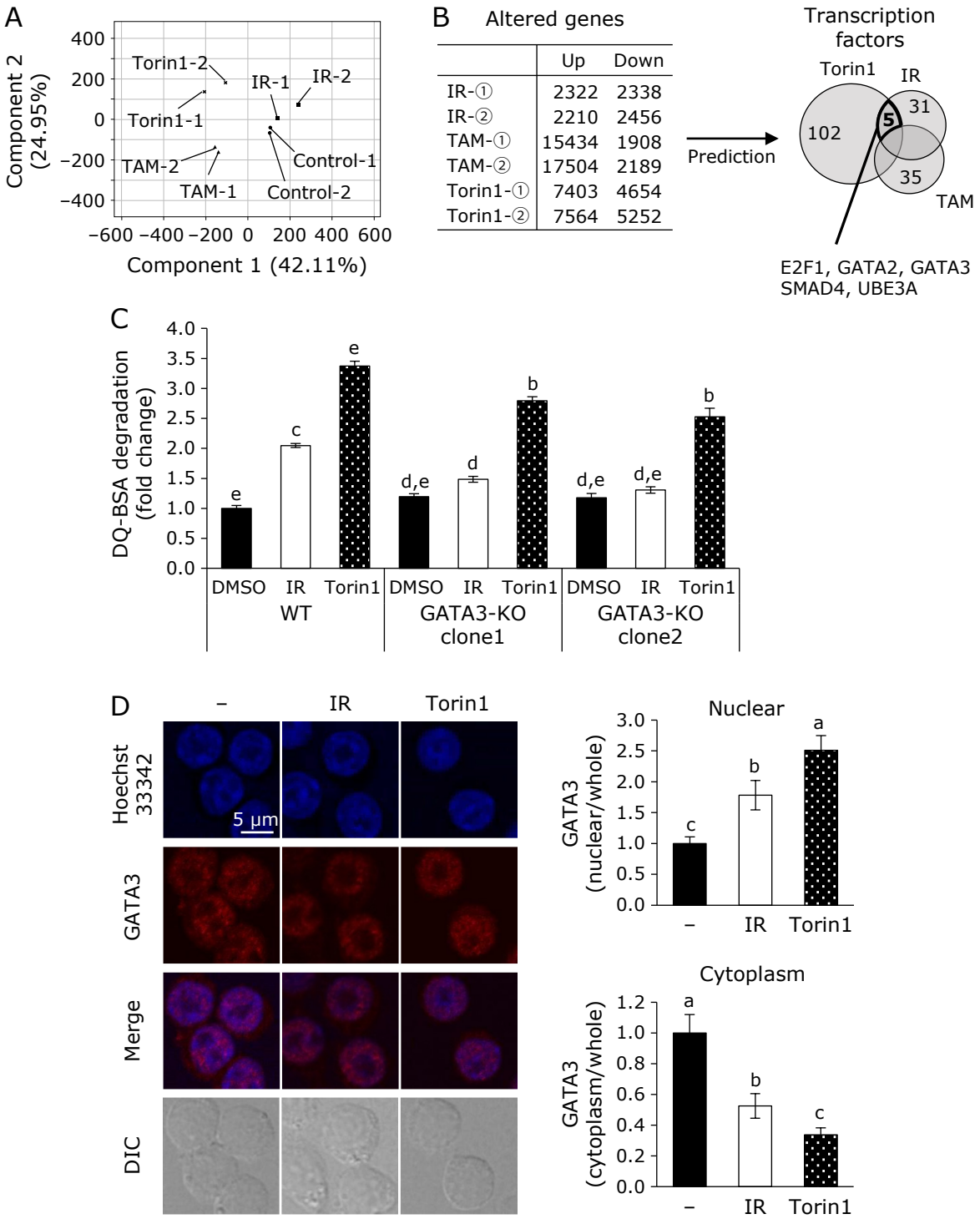

Fig. 1. A comprehensive search for the transcription factors regulating the endosomal–lysosomal system. (A, B) J774.1 cells were treated with IR (10 μM), TAM (10 μM), or Torin1 (1 μM) for 6 h, and microarray analysis was performed. (A) Principal component analysis of gene expression coordinates describes 71% of the total variation. (B) The table shows the numbers of genes altered (fold changes >1.5) by each treatment. Transcription factors affected by each treatment were predicted and shown in Venn diagrams. (C) Cells (WT, *GATA3*-KO clone1, or *GATA3*-KO clone2) were treated with IR or Torin1 for 24 h, and a DQ-BSA degradation assay was performed. The graphs indicate the fold changes compared to wild-type, untreated cells. ($n = 5$). (D) Cells were treated with IR or Torin1 for 2 h and subjected to immunofluorescence analysis using anti-GATA3 (red) antibodies. The stained cells were imaged by microscopy using a 60× objective lens. Areas of nuclear and cytoplasmic GATA3 were quantified ($n = 11$–14) and show fold changes compared to vehicles. (C, D) Bars with different letters represent statistically significant differences among groups, according to Tukey–Kramer test ($p<0.05$). IR, isorhamnetin; TAM, tamarixetin. See color figure in the on-line version.

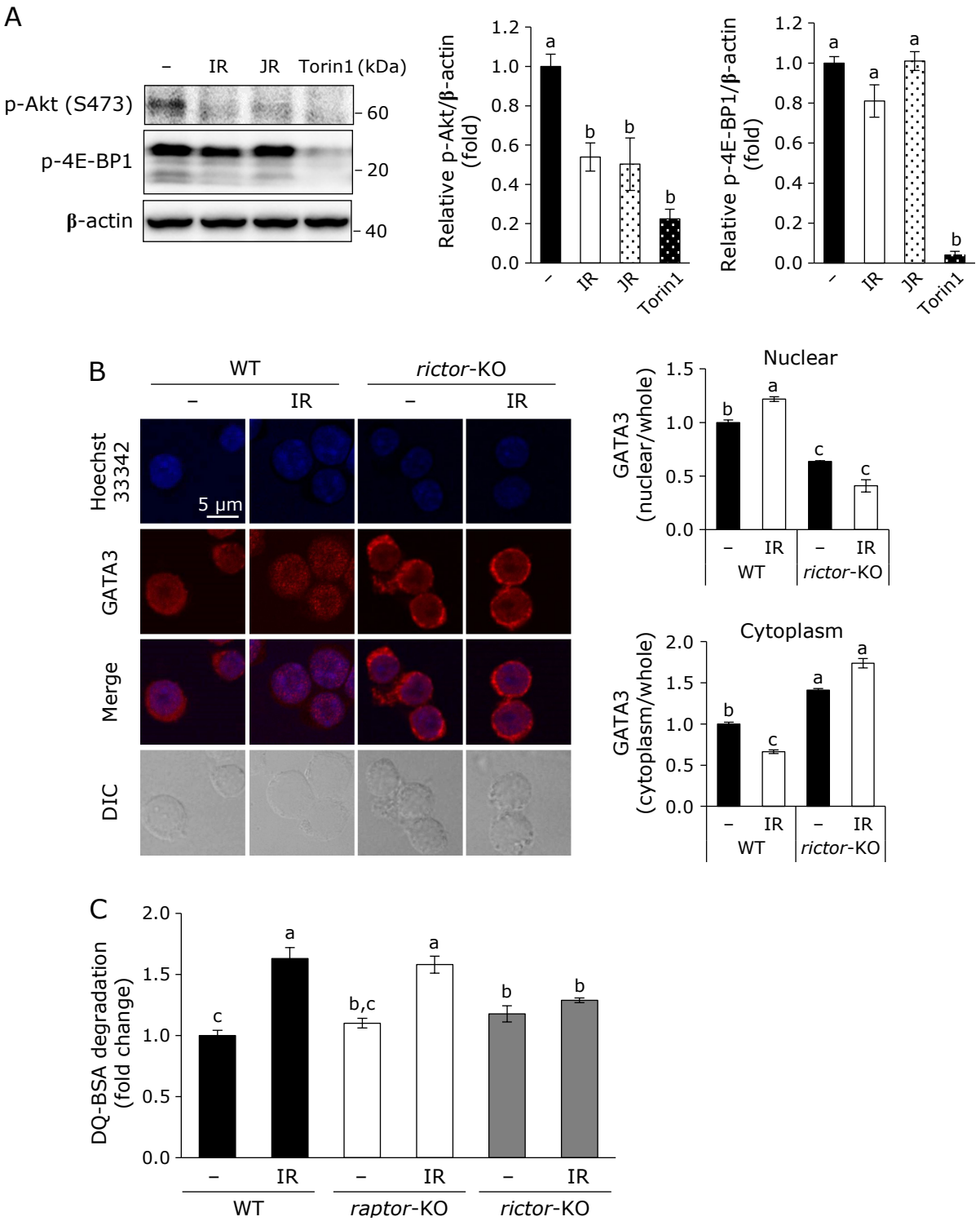

Fig. 2. Suppressing mTORC2 activity by isorhamnetin promotes GATA3 nuclear translocation and enhances endosomal–lysosomal proteolysis. (A) J774.1 cells were treated with IR (10 μM), JR-AB2-011 (10 μM), or Torin1 (1 μM) for 1 h, and phosphorylated Akt (S473) or 4E-BP1 was analyzed by Western blotting. Band intensities were quantified and show fold changes compared to vehicles ($n = 3$). (B) Cells (WT or *rictor*-KO) were treated with IR for 2 h and subjected to immunofluorescence analysis using anti-GATA3 (red) antibodies. Areas of nuclear and cytoplasmic GATA3 were quantified ($n = 9$–13) and show fold changes compared to wild-type untreated cells. (C) Cells (WT, *raptor*-KO, or *rictor*-KO) were treated with IR for 24 h, and the DQ-BSA degradation assay was performed. The bar graph shows a fold change compared to wild-type, untreated cells. ($n = 5$). (A–C) Bars with different letters represent statistically significant differences among groups, according to Tukey–Kramer test ($p<0.05$). IR, isorhamnetin. See color figure in the on-line version.

doi: 10.3164/jcbn.24-22

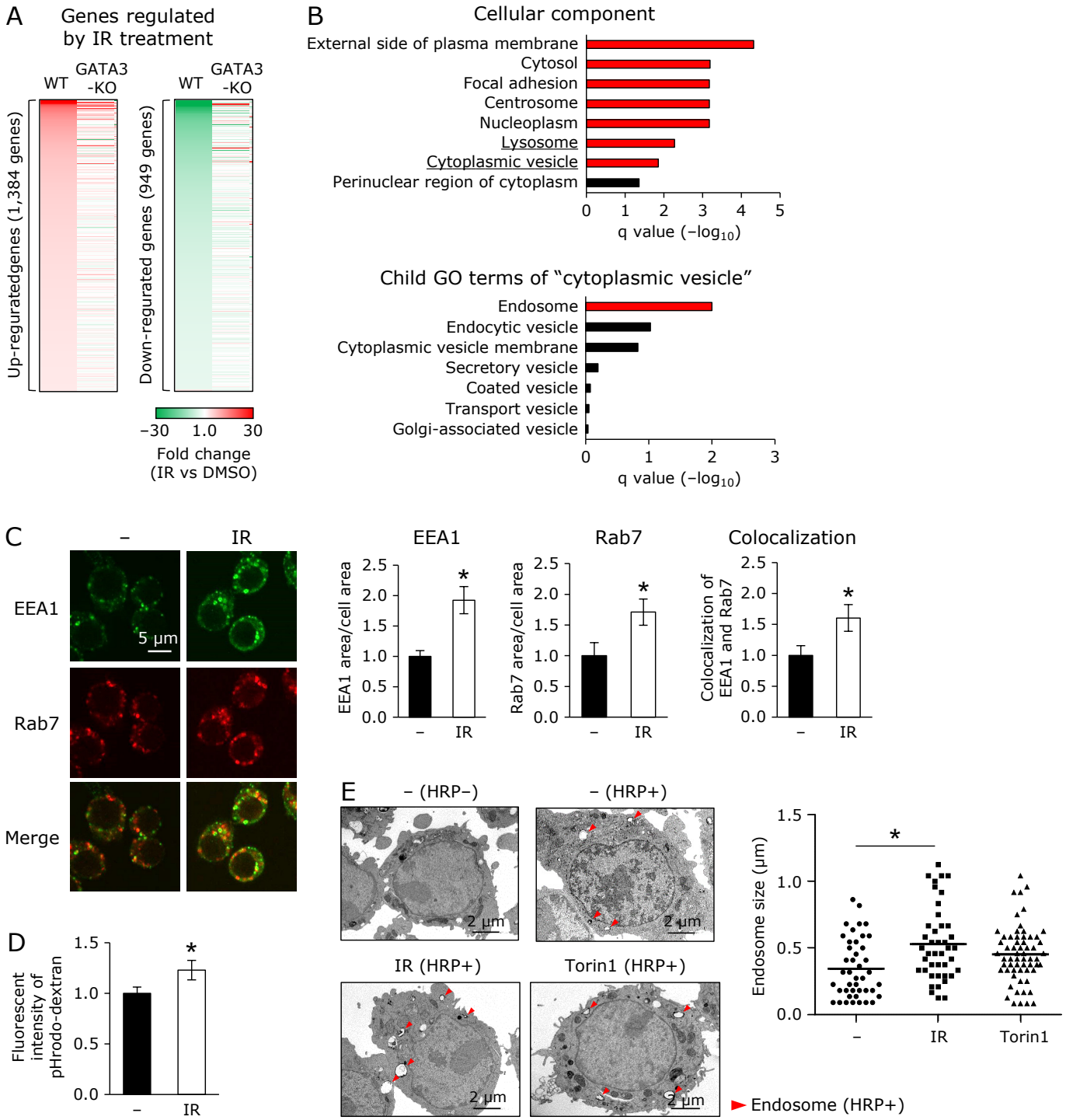

Fig. 3. GATA3 regulates gene expression related to the endosome and consequently increases endosomal formation and maturation. (A) J774.1 cells (WT, *GATA3*-KO) were treated with IR (10 μM) for 6 h, and RNA sequencing was performed. The fold changes of genes (FDR <0.05, fold changes >1.5) by IR treatment in wild-type cells were indicated in heatmaps. GATA3-dependency of genes regulated by IR is shown in chart. (B) (above) Genes altered GATA3-dependently by IR were extracted, and GO analysis was performed. The cellular component GO terms are shown in the graph below. The seven GO terms defined as more concrete terms of "cytoplasmic vesicle" are shown in the graph. The red bar denotes statistically significant enrichment (q<0.05). (C–E) J774.1 cells were treated with IR for 24 h (C) The treated cells were stimulated by DQ-BSA for 10 min to induce endocytosis, then EEA1 (green) and Rab7 (red) were co-staining and imaged using a 100× objective lens. The EEA1-positive areas, Rab7-positive area, and colocalization area were quantified and shown in the graphs (n = 14–18). (D) The treated cells were subjected to an endosomal acidification assay (n = 5). (E) The treated cells were incubated with HRP (10 mg/ml) for 10 min. and observed by an electron microscope (bar, 2 μm). HRP-positive endosomes were revealed by DAB staining (red arrows). (C, D) Bar graphs show fold changes compared to vehicles. (C–E) * indicate significant differences by the Tukey–Kramer test (p<0.05). IR, isorhamnetin. See color figure in the on-line version.

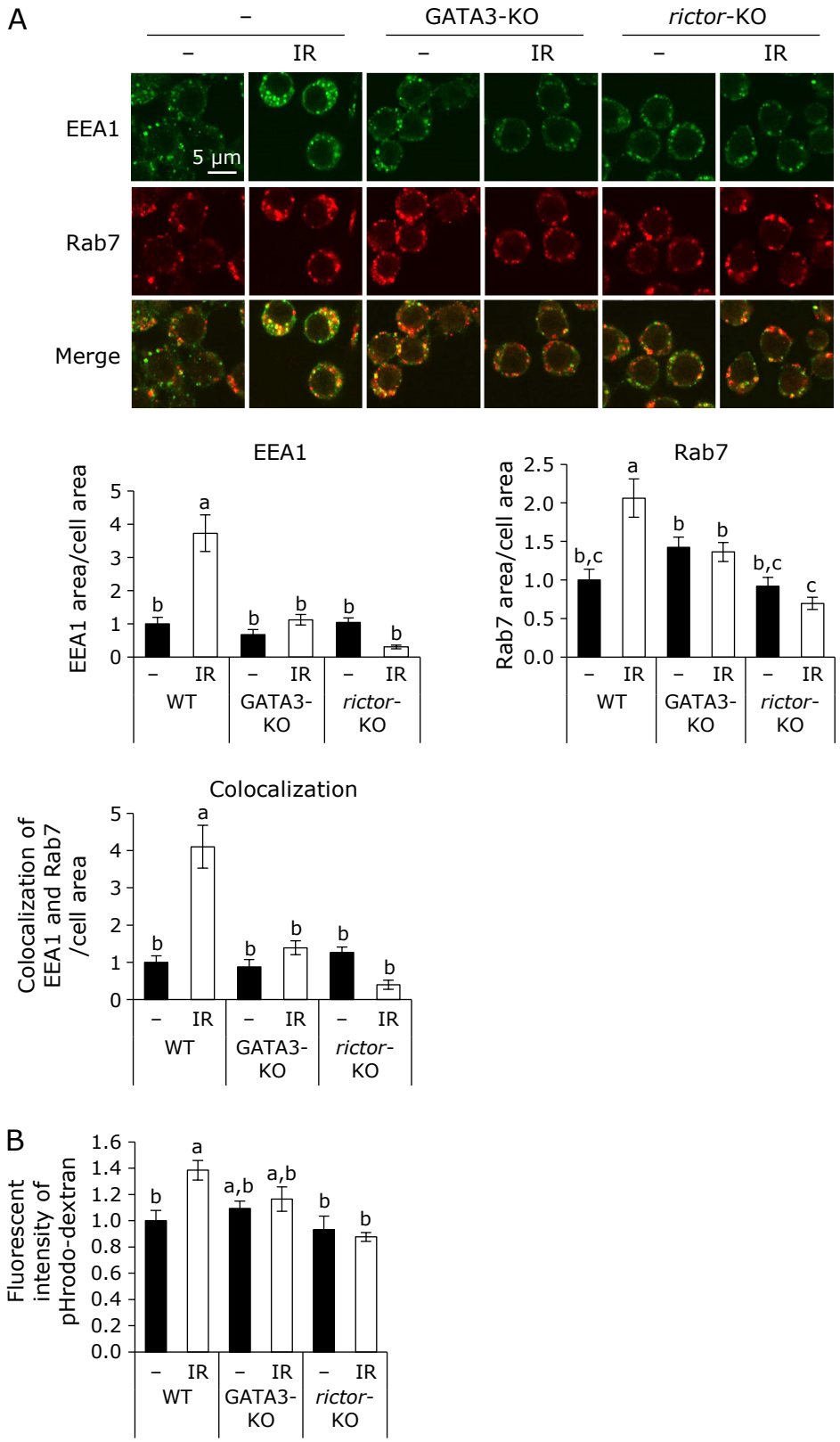

Fig. 4. mTORC2–GATA3 axis regulates endosomal formation and maturation. (A and B) J774.1 cells (WT, *GATA3*-KO, or *rictor*-KO) were treated with IR (10 μM) for 24 h. (A) The treated cells were stimulated by DQ-BSA for 10 min to induce endocytosis. Subsequently, EEA1 (green) and Rab7 (red) were co-stained and imaged using a 100× objective lens. The EEA1-positive areas, Rab7-positive area, and colocalization area were quantified (n = 16–20). (B) The treated cells were subjected to an endosomal acidification assay (n = 5). (A, B) Bar graphs show fold changes compared to wild-type, untreated cells. Bars with different letters represent statistically significant differences among groups, according to Tukey–Kramer test (p<0.05). IR, isorhamnetin. See color figure in the on-line version.

doi: 10.3164/jcbn.24-22

mTORC2–GATA3 signal regulates endosomal formation and maturation. Finally, we investigated whether the mTORC2–GATA3 axis was involved in the enhancement of endosome formation and maturation by isorhamnetin. First, we observed the impact of *GATA3* or *rictor*-knockout on early endosomes, late endosomes, and endosomes in the middle of the conversion from early to late endosomes and found that isorhamnetin failed to increase the endosome area in *GATA3* or *rictor*-deficient cells (Fig. 4A). The effects of isorhamnetin on endosomal acidification were attenuated in *rictor*-deficient cells, similar to *GATA3*-knockout cells (Fig. 4B). These data indicate that the mTORC2–GATA3 axis plays a critical role in isorhamnetin-induced endosome formation and maturation.

Discussion

We employed an informatics approach and genome editing techniques to illustrate the crucial role of the mTORC2–GATA3 axis in controlling endosomal–lysosomal degradation by regulating endosomal formation and maturation.

GATA3, a transcription factor necessary for cell differentiation in various tissues such as T cells, neurons, and adipocytes, also contributes to M2 macrophage polarization in monocytic cell lines. Despite its known roles, the involvement of GATA3 in the endosomal–lysosomal system has not been explored until now, and our data provide novel insights. During M2 macrophage polarization, IL-4 induces JAK/STAT6 signaling, activating the transcription of M2 marker genes, including *Arg1*, *CD206*, and *GATA3*.[20] GATA3, in turn, induces *IL-4* expression, creating a positive feedback loop.[21] Notably, full activation of JAK/STAT6 signaling necessitates endocytosis of the IL-4 receptor, suggesting that GATA3 activates endocytosis for efficient transduction of this signaling pathway.[22]

mTOR exists in two distinct complexes (mTORC1 and mTORC2), each catalyzing the phosphorylation of different substrates.[23] While mTORC1 controls lysosomal biogenesis and cellular uptake of extracellular substrates,[16,24] our study yielded consistent results (Supplemental Fig. 3A and B*). Interestingly, we demonstrated that pharmacological suppression of mTORC2 activity promotes endosome formation and maturation. These findings suggest a cooperative role of mTORC1 and mTORC2 in fully activating the endosomal–lysosomal system. In a recent report, isorhamnetin was identified as a potent enhancer of autophagic flux in HeLa and Caco-2 cells, implying the potential involvement of the mTORC2–GATA3 pathway in regulating the transport and fusion of autophagosomes during autophagy.[25] Additionally, we found that isorhamnetin strongly inhibited mTORC2 signaling, whose activity was comparable to that of JR-AB2-011, a selective mTORC2 inhibitor that blocks rictor–mTOR association.[26] The biochemical mechanism of how isorhamnetin inhibits mTORC2 activity remains unelucidated, which should be investigated in our future work.

We observed an increased EEA1-positive area and enlarged diameter of endocytic vesicles in cells treated with isorhamnetin. EEA1, an effector protein of Rab5, associates with the endosomal membrane under the influence of active Rab5 promoting early endosome fusion.[27,28] Macrophages expressing constitutively active Rab5 (Q79L) exhibit giant endosomes due to enhanced endosome–endosome fusion.[29] These observations suggest that isorhamnetin contributes to the activation of Rab5 and the recruitment of EEA1 to endosomes, facilitating endosome fusion for efficient transport to lysosomes. Despite the enlargement of endosomes observed in conditions of lysosomal dysfunction, such as neurological disorders,[30] isorhamnetin, as evidenced by the DQ-BSA assay, promotes protein degradation, contrary to our initial hypothesis.

When orally administered to ApoE-knockout mice at 20 mg/kg weight for eight weeks, isorhamnetin reduced atherosclerotic plaque size in the aortic valve and proximal aorta.[31] The augmented endosomal–lysosomal system in macrophages may contribute to its anti-atherosclerotic activity, though the authors concluded that isorhamnetin attenuated oxidative stress by activating Nrf2, resulting in suppressed macrophage apoptosis. Notably, isorhamnetin is a serum metabolite of quercetin, abundant in edible plants like onions and apples.[18] In mice fed a diet containing 2 mg/g of quercetin for six weeks, the serum concentration of isorhamnetin reaches approximately 2 μM.[32] Importantly, quercetin administered to ApoE-knockout mice also reduces atherosclerotic lesions.[33] These findings suggest that quercetin's *in vivo* effects may be partly dependent on the activation of endosomal–lysosomal degradation by isorhamnetin.

In summary, our results indicate that isorhamnetin modulates the mTORC2–GATA3 axis to enhance endosome formation and maturation, regulating the clearance of abnormal extracellular macromolecules in J774.1 cells. While cellular uptake and lysosomal digestion controlled by the mTORC1–TFEB axis have been studied, cargo transport controlled by the mTORC2–GATA3 axis may be a crucial pharmacological target for promoting the endosomal–lysosomal degradation of extracellular macromolecules.

Author Contributions

Study concept and design, KOhnishi, MS, and YT; Acquisition of data, MS, SY, EH, and TF; Analysis and interpretation of data, MS, KOhnishi, and AO; Writing – original draft, MS and KOhnishi; Writing – review and editing, MM, HO, KOhashi, TH, HY-O, and YT; Statistical analysis, MS; Funding acquisition, MS, KOhnishi, YT, and KOhashi; Technical support, KH and SY; Material support, EI, SI, and TH; Study supervision, KOhnishi and YT.

Acknowledgments

We thank the Fujii Memorial Institute of Medical Sciences for sharing their Operetta High-Content Imaging System. We also thank the Support Center for Advanced Medical Sciences, Tokushima University Graduate School of Biomedical Sciences, for the use of confocal microscopy and transmission electron microscopy, and the Institute of Advanced Medical Sciences, Tokushima University, for the use of the CLC Genomics Workbench. We sincerely thank Dr. Takeshi Nikawa for allowing us to use the fluorescence microscope. We thank Ms. Satoko Nakano, Ms. Rumiko Masuda, Ms. Akiko Uebanso, and Ms. Megumi Abe for their support and encouragement. This study was supported by the joint research program of the Institute for Molecular and Cellular Regulation, Gunma University (Project Number 20014), and the Japan Society for the Promotion of Science (Grant Nos. 22KJ2350, 20J14993, 18K14422, 20K19675, and 19H04053).

Abbreviations

4E-BP1	eukaryotic translation initiation factor 4E binding protein 1
EEA1	early endosome antigen 1
GATA3	GATA-binding protein 3
GO	gene ontology
mTOR	mammalian target of rapamycin
Rab	Ras-related protein in the brain
raptor	regulatory-associated protein of mTOR
rictor	rapamycin-insensitive companion of mTOR
TFEB	transcription factor EB

Data Availability

Microarray and RNA-sequencing data were deposited in

*See online. https://doi.org/10.3164/jcbn.24-22

NCBI's Gene Expression Omnibus under the accession numbers GSE166821 and GSE167009. All other data were included in this article.

Conflict of Interest

No potential conflicts of interest were disclosed.

References

1 Wang M, Kaufman RJ. Protein misfolding in the endoplasmic reticulum as a conduit to human disease. *Nature* 2016; **529**: 326–335.
2 Ohkubo Y, Nakato R, Uehara T. Regulation of unfolded protein response via protein *S*-nitrosylation. *Yakugaku Zasshi* 2016; **136**: 801–804.
3 Spencer E, Rosengrave P, Williman J, Shaw G, Carr AC. Circulating protein carbonyls are specifically elevated in critically ill patients with pneumonia relative to other sources of sepsis. *Free Radic Biol Med* 2022; **179**: 208–212.
4 Gill V, Kumar V, Singh K, Kumar A, Kim JJ. Advanced glycation end products (AGEs) may be a striking link between modern diet and health. *Biomolecules* 2019; **9**: 888.
5 Paul D, Stern O, Vallis Y, Dhillon J, Buchanan A, McMahon H. Cell surface protein aggregation triggers endocytosis to maintain plasma membrane proteostasis. *Nat Commun* 2023; **14**: 947.
6 Pohl C, Dikic I. Cellular quality control by the ubiquitin-proteasome system and autophagy. *Science* 2019; **366**: 818–822.
7 Menzies FM, Fleming A, Caricasole A, *et al*. Autophagy and neurodegeneration: pathogenic mechanisms and therapeutic opportunities. *Neuron* 2017; **93**: 1015–1034.
8 Luo R, Su LY, Li G, *et al*. Activation of PPARA-mediated autophagy reduces Alzheimer disease-like pathology and cognitive decline in a murine model. *Autophagy* 2020; **16**: 52–69.
9 Nakai A, Yamaguchi O, Takeda T, *et al*. The role of autophagy in cardiomyocytes in the basal state and in response to hemodynamic stress. *Nat Med* 2007; **13**: 619–624.
10 Pierdominici M, Vomero M, Barbati C, *et al*. Role of autophagy in immunity and autoimmunity, with a special focus on systemic lupus erythematosus. *FASEB J* 2012; **26**: 1400–1412.
11 Alers S, Löffler AS, Wesselborg S, Stork B. Role of AMPK-mTOR-Ulk1/2 in the regulation of autophagy: cross talk, shortcuts, and feedbacks. *Mol Cell Biol* 2012; **32**: 2–11.
12 Yamamoto H, Zhang S, Mizushima N. Autophagy genes in biology and disease. *Nat Rev Genet* 2023; **24**: 382–400.
13 Hu YB, Dammer EB, Ren RJ, Wang G. The endosomal-lysosomal system: from acidification and cargo sorting to neurodegeneration. *Transl Neurodegener* 2015; **4**: 18.
14 Cullen PJ, Steinberg F. To degrade or not to degrade: mechanisms and significance of endocytic recycling. *Nat Rev Mol Cell Biol* 2018; **19**: 679–696.
15 Sergin I, Evans TD, Zhang X, *et al*. Exploiting macrophage autophagy-lysosomal biogenesis as a therapy for atherosclerosis. *Nat Commun* 2017; **8**: 15750.
16 Nnah IC, Wang B, Saqcena C, *et al*. TFEB-driven endocytosis coordinates MTORC1 signaling and autophagy. *Autophagy* 2019; **15**: 151–164.
17 Sakai M, Ohnishi K, Masuda M, *et al*. Isorhamnetin, a 3'-methoxylated flavonol, enhances the lysosomal proteolysis in J774.1 murine macrophages in a TFEB-independent manner. *Biosci Biotechnol Biochem* 2020; **84**: 1221–1231.
18 Cao J, Chen W, Zhang Y, Zhang Y, Zhao X. Content of selected flavonoids in 100 edible vegetables and fruits. *Food Sci Technol Res* 2010; **16**: 395–402.
19 Martell JD, Deerinck TJ, Lam SS, Ellisman MH, Ting AY. Electron microscopy using the genetically encoded APEX2 tag in cultured mammalian cells. *Nat Protoc* 2017; **12**: 1792–1816.
20 Shapouri-Moghaddam A, Mohammadian S, Vazini H, *et al*. Macrophage plasticity, polarization, and function in health and disease. *J Cell Physiol* 2018; **233**: 6425–6440.
21 Ho IC, Tai TS, Pai SY. GATA3 and the T-cell lineage: essential functions before and after T-helper-2-cell differentiation. *Nat Rev Immunol* 2009; **9**: 125–135.
22 Kurgonaite K, Gandhi H, Kurth T, *et al*. Essential role of endocytosis for interleukin-4-receptor-mediated JAK/STAT signalling. *J Cell Sci* 2015; **128**: 3781–3795.
23 Battaglioni S, Benjamin D, Wälchli M, Maier T, Hall MN. mTOR substrate phosphorylation in growth control. *Cell* 2022; **185**: 1814–1836.
24 Settembre C, Di Malta C, Polito VA, *et al*. TFEB links autophagy to lysosomal biogenesis. *Science* 2011; **332**: 1429–1433.
25 Ohnishi K, Yano S, Fujimoto M, *et al*. Identification of dietary phytochemicals capable of enhancing the autophagy flux in HeLa and Caco-2 human cell lines. *Antioxidants (Basel)* 2020; **9**: 1193.
26 Benavides-Serrato A, Lee J, Holmes B, *et al*. Specific blockade of Rictor-mTOR association inhibits mTORC2 activity and is cytotoxic in glioblastoma. *PLoS One* 2017; **12**: e0176599.
27 Haas AK, Fuchs E, Kopajtich R, Barr FA. A GTPase-activating protein controls Rab5 function in endocytic trafficking. *Nat Cell Biol* 2005; **7**: 887–893.
28 Christoforidis S, McBride HM, Burgoyne RD, Zerial M. The Rab5 effector EEA1 is a core component of endosome docking. *Nature* 1999; **397**: 621–625.
29 Duclos S, Corsini R, Desjardins M. Remodeling of endosomes during lysosome biogenesis involves 'kiss and run' fusion events regulated by rab5. *J Cell Sci* 2003; **116 (Pt 5)**: 907–918.
30 Kaur G, Lakkaraju A. Early endosome morphology in health and disease. *Adv Exp Med Biol* 2018; **1074**: 335–343.
31 Luo Y, Sun G, Dong X, *et al*. Isorhamnetin attenuates atherosclerosis by inhibiting macrophage apoptosis via PI3K/AKT activation and HO-1 induction. *PLoS One* 2015; **10**: e0120259.
32 Boesch-Saadatmandi C, Egert S, Schrader C, *et al*. Effect of quercetin on paraoxonase 1 activity—studies in cultured cells, mice and humans. *J Physiol Pharmacol* 2010; **61**: 99–105.
33 Shen Y, Ward NC, Hodgson JM, *et al*. Dietary quercetin attenuates oxidant-induced endothelial dysfunction and atherosclerosis in apolipoprotein E knockout mice fed a high-fat diet: a critical role for heme oxygenase-1. *Free Radic Biol Med* 2013; **65**: 908–915.

doi: 10.3164/jcbn.24-22